ADVANCED MATERIALS
www.advmat.de

Single Layer Silk and Cotton Woven Fabrics for Acoustic Emission and Active Sound Suppression

*Grace H. Yang, Jinuan Lin, Henry Cheung, Guanchun Rui, Yongyi Zhao, Latika Balachander, Taigyu Joo, Hyunhee Lee, Zachary P. Smith, Lei Zhu, Chu Ma, and Yoel Fink**

Whether intentionally generating acoustic waves or attempting to mitigate unwanted noise, sound control is an area of challenge and opportunity. This study investigates traditional fabrics as emitters and suppressors of sound. When attached to a single strand of a piezoelectric fiber actuator, a silk fabric emits up to 70 dB of sound. Despite the complex fabric structure, vibrometer measurements reveal behavior reminiscent of a classical thin plate. Fabric pore size relative to the viscous boundary layer thickness is found—through comparative fabric analysis—to influence acoustic-emission efficiency. Sound suppression is demonstrated using two distinct mechanisms. In the first, direct acoustic interference is shown to reduce sound by up to 37 dB. The second relies on pacifying the fabric vibrations by the piezoelectric fiber, reducing the amplitude of vibration waves by 95% and attenuating the transmitted sound by up to 75%. Interestingly, this vibration-mediated suppression in principle reduces sound in an unlimited volume. It also allows the acoustic reflectivity of the fabric to be dynamically controlled, increasing by up to 68%. The sound emission and suppression efficiency of a 130 µm silk fabric presents opportunities for sound control in a variety of applications ranging from apparel to transportation to architecture.

1. Introduction

Sound, an omnipresent sensory stimulator, holds significant relevance in the human experience, as it continually engages our auditory and mental faculties. The importance of sound is underscored by its dual nature, serving as both a vital tool for communication and a potential source of harm, exemplified by the pervasive issue of noise pollution.[1] Considered to be a public health issue by the World Health Organization, unwanted noise can have harmful health effects on people who are chronically exposed to it.[1–5] In the US alone, an estimated 145 million people are exposed to hazardous noise levels.[5] To suppress noise levels, both active and passive solutions are used.

Active noise reduction realizes suppression of sound in a small volume[6] and has become a significant area of application for headphones and earbuds, where

G. H. Yang, T. Joo, H. Lee, Z. P. Smith
Department of Chemical Engineering
Massachusetts Institute of Technology (MIT)
Cambridge, MA 02139, USA

J. Lin, C. Ma
Department of Electrical and Computer Engineering
University of Wisconsin–Madison
Madison, WI 53706, USA

H. Cheung, Y. Zhao, Y. Fink
Department of Electrical Engineering and Computer Science
Massachusetts Institute of Technology
Cambridge, MA 02139, USA
E-mail: yoel@mit.edu

G. Rui, L. Zhu
Department of Macromolecular Science and Engineering
Case Western Reserve University
Cleveland, OH 44106, USA

L. Balachander
Textiles Department
Rhode Island School of Design
Providence, RI 02903, USA

Y. Fink
Department of Materials Science and Engineering
Massachusetts Institute of Technology
Cambridge, MA 02139, USA

Y. Fink
Research Laboratory of Electronics
Massachusetts Institute of Technology
Cambridge, MA 02139, USA

The ORCID identification number(s) for the author(s) of this article can be found under https://doi.org/10.1002/adma.202313328

DOI: 10.1002/adma.202313328

only a small quiet zone near the eardrum is needed. Larger scale volumetric sound suppression, e.g., in a room, is primarily done through passive approaches, such as reflection of sound using materials with high acoustic impedance or absorption of sound typically done with fibrous structures or foams.[7,8] Despite their ubiquity, these materials suffer from low performance at low frequencies, often necessitating layers of soundproofing material that are 15–100 mm thick.[8] Moreover, the aesthetic and environmental implications are significant as many of these materials are made of hydrocarbons. It is estimated that the volume of fibrous soundproofing is more than 5 billion cubic meters and is an ≈$12 billion market.[9] The absence of compact, lightweight, and efficient sound suppression materials constitutes a limitation, motivating an unmet need for thin and visually aesthetic sound barriers.

This study aims to initially identify ways a traditional fabric can be engineered to broadcast sound. Subsequently, two different mechanisms are explored by which a thin fabric can efficiently suppress sound. The first involves emitting an out-of-phase acoustic wave that destructively interferes with the unwanted sound. This is commonly referred to as "active noise cancellation," and we will refer to it as "direct acoustic suppression." The second approach relies on the fact that much of the sound that we hear emanates from or is transmitted through vibrating solid structures.[10] Thus, the second mechanism suppresses the vibrations in the mediating domain, in this case the fabric, to prevent the sound from being transmitted. This second sound reduction mechanism will be referred to as "vibration-mediated suppression."

We present the characterization of a fabric which contains a single piezoelectric fiber actuator that can serve as a sound emitter for direct acoustic suppression or vibration-mediated suppression. The fiber is sewn into three different fabrics and attached to a membrane to create sound emitters, whose generated sound pressure level (SPL) and vibration patterns are studied to better understand performance. A finite element model in COMSOL validates the experimental results. The fabric emitter demonstrates effective sound emission and direct acoustic suppression. Finally, the fabric achieves a 75% decrease in sound as its vibrations are suppressed up to 95%, and it is controlled to modulate acoustic reflectivity.

2. Fabric Sound Emission in Hanging State and with Fixed Boundary Conditions

Research around flexible or soft acoustic transducers is a growing area of interest for acoustic modulation, pressure sensing, and sound control.[11–14] To that end, thermally drawn piezoelectric polymer-based fibers have been developed and improved for enhanced sensitivity in various applications.[15–17] This study begins with the production of a sound-emitting fabric, involving the initial fabrication of a piezoelectric fiber[17] that is subsequently secured to the surface of the fabric. The fiber device in this study is fabricated using thermal drawing, as previously described.[17] The preform (25 × 14 × 200 mm) consists of a piezoelectric composite domain, sandwiched by two electrodes and encapsulated by an elastomeric cladding. During the draw, these materials are heated and coflow to form a fiber with a preserved cross-sectional geometry, as shown in **Figure 1**a–c (Figure S1, Supporting Information). The piezoelectric domain consists of the copolymer poly(vinylidene fluoride–trifluoroethylene) [P(VDF–TrFE)] 70/30 by molar ratio, containing 20 wt% 200 nm piezoelectric barium titanate ceramic particles. The electrodes are carbon-loaded polyethylene with two continuous copper wires that are embedded in each electrode during the draw using a process known as convergence.[17] These layers are surrounded by poly(styrene-*b*-(ethylene-*co*-butylene)-*b*-styrene) (SEBS) cladding. The final fiber is dozens of meters long and has a cross-section of about 1.25 mm by 0.65 mm, with a piezoelectric domain thickness of 30 µm. The high d_{31} piezoelectric coefficient of the fiber[17] which results from its poling process (Figure 1d,e and Figure S2 (Supporting Information)) and composition leads—upon voltage application (Figure 1f)—to axial bending of the fiber, which in turn creates mechanical waves in the fabric that give rise to acoustic pressure waves.

Specifically, a 6.7 cm fiber is sewn onto an 8 cm diameter circular, plain-weave silk fabric that is 130 µm thick. This fabric is mounted in a frame so that all the edges are fixed using the method shown in Figure S3 (Supporting Information) to control the boundary conditions for reproducibility. To serve as a reference, a fiber of the same length is attached using a thin layer of adhesive to a 50 µm thick Mylar circular membrane that is 8 cm in diameter and mounted following the same procedure shown in Figure S3 (Supporting Information). A circular geometry with fixed edges was chosen in order to control the boundary conditions. However, for many fabrics encountered in daily life, rectangular shapes and multiple free edges are common. Therefore, a rectangular silk fabric sample in a hanging state was tested and compared. The performance of an 8 cm square fabric with a 6.7 cm fiber sewn onto the center was compared to that of the silk-in-frame emitter and Mylar-in-frame emitter (**Figure 2**a,b).

Here, the fabrics and membrane were recorded emitting multifrequency sound, specifically "Air" (J. S. Bach). The reference microphone was placed 2.5 cm away from the fabric or membrane, and the sound was recorded over the duration of the song to compare the SPLs and the frequency content of the sound emitted by the various samples (Figure 2c,d). Given their different mechanical properties (Mylar compared to silk) and boundary conditions (hanging compared to fixed), different vibrational modes of the samples will be excited, but they still show fidelity to the original frequency content, albeit with differing intensities depending on the mode shape and displacement.

All three samples emit sound above the noise floor for the duration of the song. The Mylar outperforms both of the silk fabrics, with an average SPL 5.8 dB higher than that of the silk-in-frame and 16.6 dB higher than that of the hanging silk. Additionally, sensitivity measurements show that the Mylar-in-frame has a comparable, if not better, performance than other membrane loudspeakers reported in literature (Figure S4, Supporting Information).[18–27]

The spectrograms of the original audio file and the recordings from a commercial speaker, the Mylar in frame, the silk in frame, and the hanging silk were also compared (Figure 2d). The amplitude of the waveform was normalized before creating the spectrogram so that comparisons of frequency content can be made more easily. Oftentimes, commercial loudspeakers have multiple cones—larger cones for lower frequencies and smaller cones for

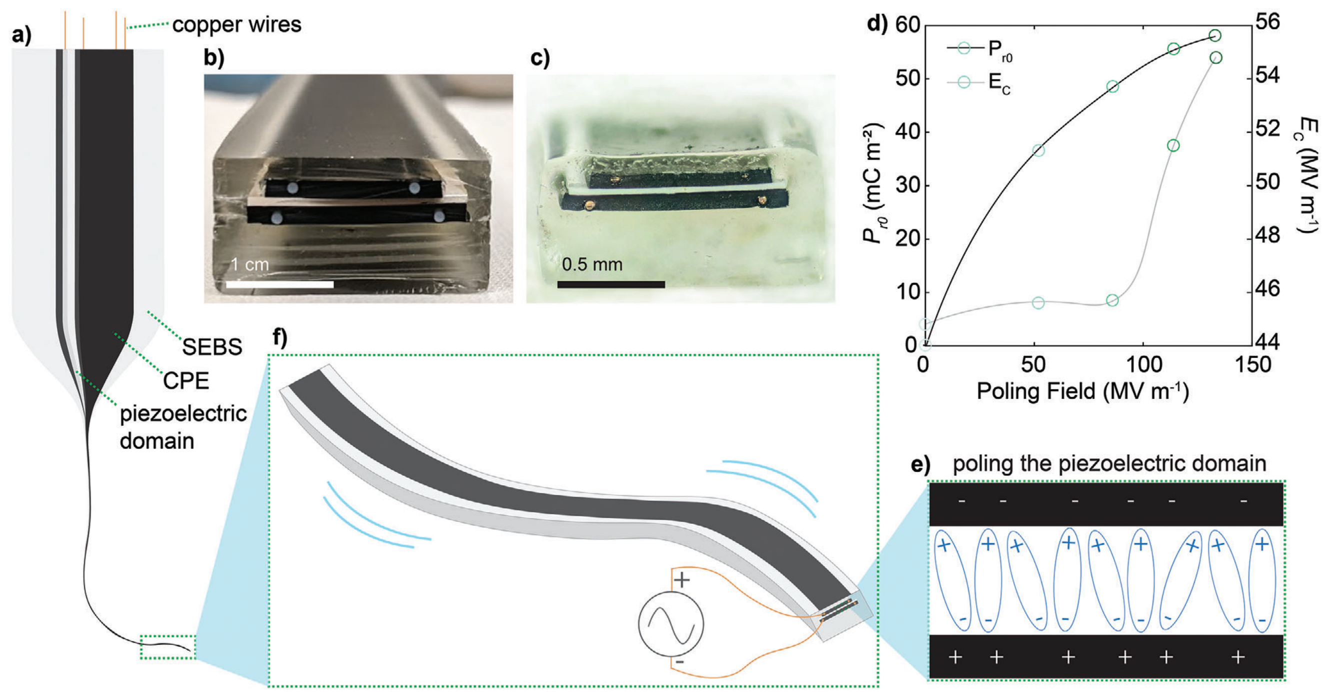

Figure 1. a) Schematic of the preform being drawn into fiber. b) The cross-section of the preform is ≈2.5 cm × 1.4 cm. c) The cross-section of the fiber is ≈1.25 mm × 0.7 mm. d) The dependence of the permanent remanent polarization P_{r0} and the coercive electric field E_C on the DC electric poling field, e) which is applied after drawing the fiber to orient the dipoles. f) Mechanical motion is induced by an AC voltage applied to the fiber.

higher frequencies. For the commercial loudspeaker, the output of the larger cone was recorded. There is a clear cutoff around 3 kHz, showing how the cone size limits the frequency response. The response of the Mylar begins to taper off at 4 kHz, similar to the original audio. Although they have a lower SPL, both of the silk fabrics show preserved frequency content up to 10 kHz, suggesting efficient generation of sound at the higher frequencies.

3. Fabric Properties Influencing Emission

A 6.7 cm fiber is sewn onto an 8 cm diameter canvas sample (**Figure 3a**), which is mounted into a circular frame as before. The canvas is a plain weave fabric composed of high denier cotton yarns in a tight weave (bulk density = 0.687 g cm^{-3}, thickness = 1.15 mm). The Young's modulus at low displacements, up to 10 µm, is measured to be 180 MPa. To characterize the fabric emitter, 1 kV peak-to-peak is applied to the fiber at each frequency, and the SPL is measured using a reference microphone at 2.5 cm. The displacement of the surface of the fabric is measured using a scanning laser vibrometer. The vibrometer measurements reveal the fabric vibration patterns generated by the fiber device at each frequency, and the average magnitude of velocity (i.e., speed) over the surface of the fabric is calculated.

The fabric emitter generates audible sound over the frequency range tested, 100 Hz to 5 kHz (Figure 3b). For reference, human speech is generally in the range of 300 Hz to 3.4 kHz, with 60 dB considered as a conversational volume.[28] The canvas loudspeaker produces sound up to 69.4 dB (Figure 3b). Far field measurements are shown in Figure S5 (Supporting Information).

The frequency response of both the SPL and the average speed of the fabric have multiple resonant peaks, which are characteristic of thin-film acoustic actuators,[24,29] including the tympanic membrane itself.[30] Shown side-by-side (Figure 3b), the peaks of the average speed of the fabric align well with the peaks of the SPL at a given frequency. As the resonant peaks show, higher speeds of the fabric result in higher generated SPLs. This follows from equations for the axial pressure amplitude radiating from a plane rigid circular piston, which show pressure amplitude to be proportional to speed.[8] The power draw of the fiber increases with frequency as the capacitive reactance is inversely proportional to frequency, and thus higher frequencies result in higher power draw (Figure S6, Supporting Information).[31] With the increased power, the average speed increases, which leads to the SPL trending higher over the frequency range.

Despite the complex structure of the fabric and the fiber coupled to its surface, the shapes of the exhibited vibration modes match those of a theoretical thin circular plate with fixed edges. The vibration of a circular plate with fixed edges is a function of the thickness d, Young's modulus E, Poisson's ratio ν, and density ρ[8]

$$\frac{\partial^2 y}{\partial t^2} = -\frac{d^2 E}{12\rho\,(1 - \nu^2)}\nabla^2\left(\nabla^2 y\right) \tag{1}$$

These mechanical properties dictate the fabric's vibrational response to pressure at a particular frequency. Additionally, the specific flow resistance is a measure of how easily air can enter a porous structure, as well as the resistance that flow meets within the structure, and it is an important characteristic of porous materials in acoustic applications.[7] The specific flow resistance of canvas was measured to be 0.462 bar s m^{-1} (Figure S7, Supporting Information). It is intuitive to think that larger flow resistance

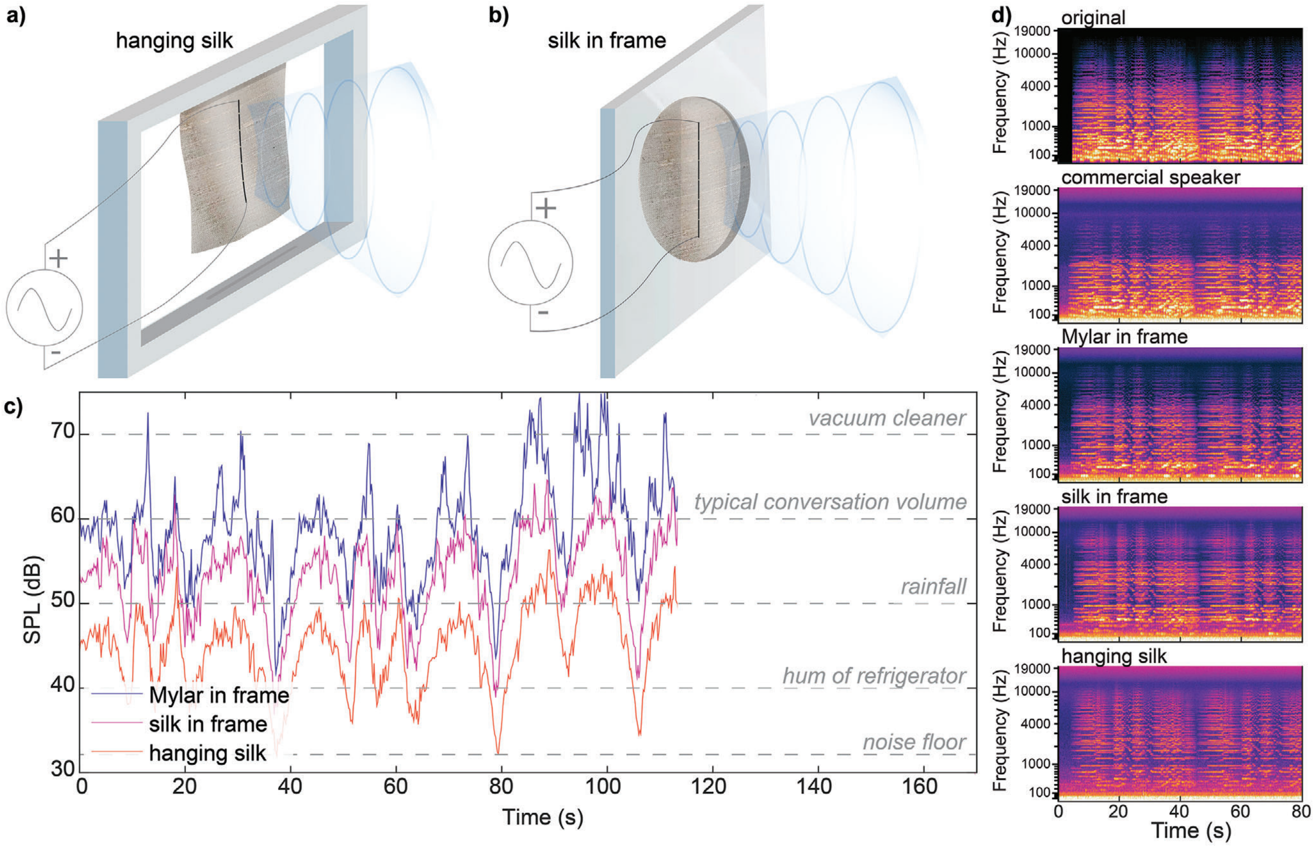

Figure 2. Silk fabric samples a) in a hanging state and b) mounted in a circular frame. The AC symbol represents the voltage supplied to each fabric. c) SPL (measured at 2.5 cm) emitted by Mylar in a frame, silk in a frame, and the hanging silk over the course of playing "Air" (Bach). Examples of sounds at various SPLs are provided for reference. d) Spectrograms of the original audio and recordings from a commercial speaker, the Mylar in a frame, the silk in a frame, and the hanging silk.

would generally lead to higher SPLs as more air would be pushed by the fabric rather than flow through the fabric, but the extent of the effect of the flow resistance is dependent on the pore size, as explained in the following section.

A finite element analysis model was constructed in COMSOL Multiphysics 6.1. Structural mechanics, acoustics, and poroelastic waves modules were used to simulate the surface displacement as well as the generated SPL. To improve our understanding of how the novel fabric emitter system behaves, we hypothesized that it generally follows the classic vibrating thin plate. If true, this establishes a foundation from which to understand and tune the behaviors of this novel system. Thus, we simulated a simplified model of the system, abstracting away the detailed microstructures of the fiber and fabric. The goal of the simulation was determining whether this simple model captures the key features and trends of the experimental observations, rather than fully recapitulating the quantitative details. The fiber on canvas was modeled as a simple block representing the fiber coupled to a thin plate representing the fabric. The model inputs were the thickness, Young's modulus, density, Poisson's ratio, porosity, specific flow resistance, and isotropic loss factor. Rather than simulating the piezoelectric transduction mechanism of the fiber, the force generated by the fiber was simplified and modeled as a background pressure field which acts as a uniform force over the area of the fabric. The simulation and experiments show a good match in the frequency response of the average speed and SPL (Figure 3b) as well as the vibrational mode shapes of the first four resonant modes (Figure 3c,d). This shows that the complex structure of the fabric with the fiber coupled to the surface follows similar behavior to a vibrating thin plate with an attached mass that is governed by key mechanical and acoustical properties. A sensitivity analysis using this simulation reveals that thinner and higher modulus substrates should lead to a higher average speeds and thus higher SPLs (Figure S8, Supporting Information). As such, these properties can be engineered to achieve higher acoustic output or change the resonant peaks as desired for specific applications.

4. Influence of Pore Size

Two plain-weave fabrics, muslin and silk, were chosen to explore how the properties related to the porosity of fabrics influence the SPL output. The muslin is a lightweight fabric (bulk density = 0.673 g cm^{-3}, thickness = 0.15 mm) composed of natural cotton fibers that are spun into staple yarns. The silk fabric is thin yet more tightly woven (bulk density = 0.615 g cm^{-3}, thickness = 0.13 mm) and composed of the natural filament fiber silk. The

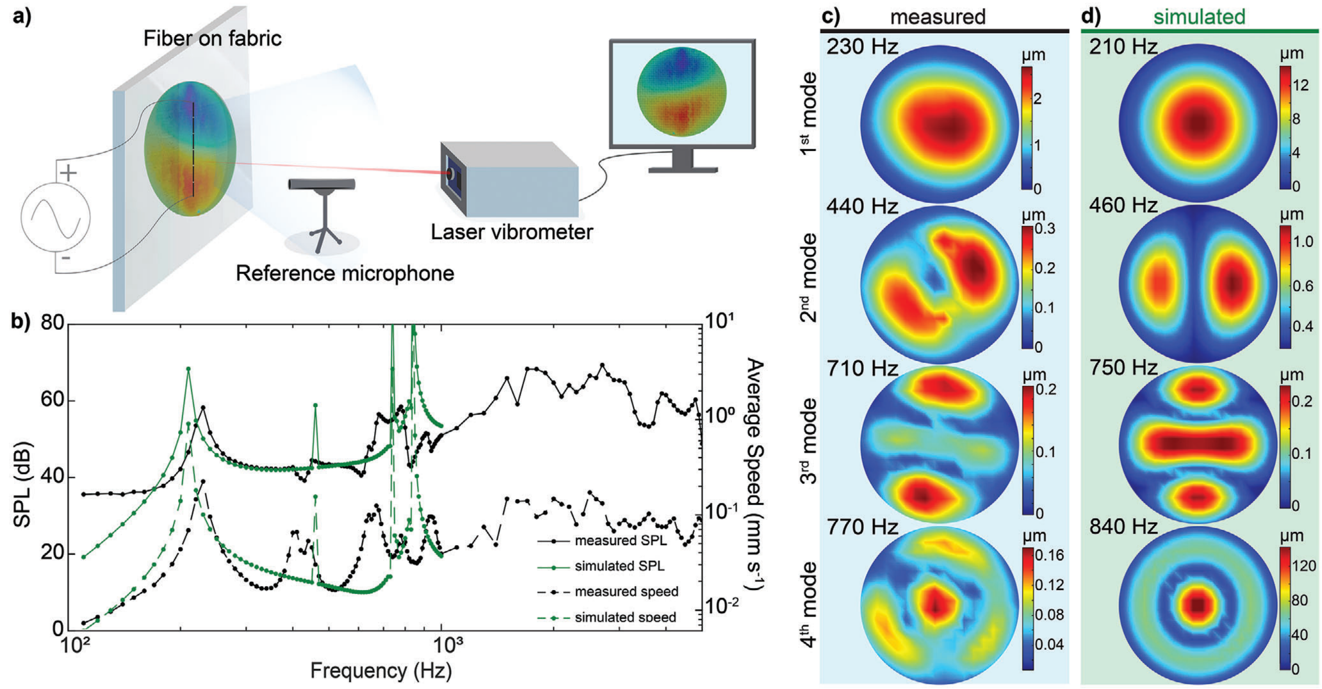

Figure 3. a) Schematic of the measurement setup for collecting SPL and velocity data from a fabric speaker in a frame. b) Measured frequency response of the average speed and SPL of the fiber-on-canvas loudspeaker and results from COMSOL simulations. The noise floor is around 35 dB. c) Measured displacement patterns compared to d) the simulated displacement patterns of the first four resonant modes.

measured Young's modulus values are 114 and 183 MPa for the muslin and silk fabrics, respectively.

As the various characteristics of fabrics are highly interdependent, it is difficult to vary a single parameter without influencing the others. For example, weaving a thicker fabric will likely require higher denier yarns which can change the pore size or porosity and bulk density. The modulus of the fabric at low strains is also determined by the interfiber friction effects, so the tightness of the weave and the yarn and constituent fiber's surfaces influence the modulus.[32] Despite this complexity, the silk and muslin fabrics are similar in most of their parameters and exhibit a similar vibrational wavelength (Figure S9, Supporting Information). Because of their similar mechanical properties, it is expected that the two would have similar sound emission behavior. Over the frequency range, both fabrics' responses are characterized by multiple resonant peaks (**Figure 4**a). The linear relationship between input power and acoustic intensity shows no harmonic distortion as the generated SPL scales linearly with power and thus input voltage (Figure 4b).[25] These two fabrics have comparable average speeds, increasing with frequency. This is expected given their similar vibrational wavelengths. However, while the SPL of the silk continues to increase with frequency, the SPL of the muslin levels off.

Where these fabrics differ is their average pore size. Based on optical microscopy images (Figure 4c,d), assuming that these pores are square, which is reasonable given the weave structure, the average pore lengths for muslin and silk are 167 and 46 µm, respectively. As a fabric vibrates in air, some of the air will be pushed, creating a pressure wave, but some of the air will flow through the pores of the fabric if they are large enough. The friction effect between the flowing air and the solid structure of the fabric gives rise to the viscous boundary layer, the thin layer of air adjacent to the solid surface of the yarns, where the effects of viscosity dominate and the flow velocity relative to the fabric gradually changes from zero (due to the nonslip condition between the solid and the air) to the free stream velocity. The viscous boundary layer δ_v is calculated using the following equation

$$\delta_v = \sqrt{\frac{\mu}{2\pi f \rho}} \tag{2}$$

where μ and ρ are the dynamic viscosity and density of air, respectively.[33] When the viscous boundary layer is greater than half of the pore length, the structure of the pores becomes mechanically invisible, and the porosity and flow resistance of the fabric do not affect the acoustics. For muslin, this condition is met at frequencies below ≈300 Hz, whereas for silk, it is met at frequencies below ≈4500 Hz (Figure 4e). We propose that over the measurement range, the silk behaves approximately as nonporous, while the muslin's large pores account for more losses. The discrepancy in the generated SPLs from the two fabrics can be explained by the larger pore size of muslin. Rather than being effectively pushed, a larger fraction of the air flows through the pores, unimpeded by the relatively thin viscous boundary layer. Additional control groups shown in Figures S10–S12 (Supporting Information) exhibit consistent results.

5. Direct Acoustic Suppression

In addition to transmitting sound (**Figure 5**a) and emitting sound (Figure 5b) for propagation, the fabric emitter can be used

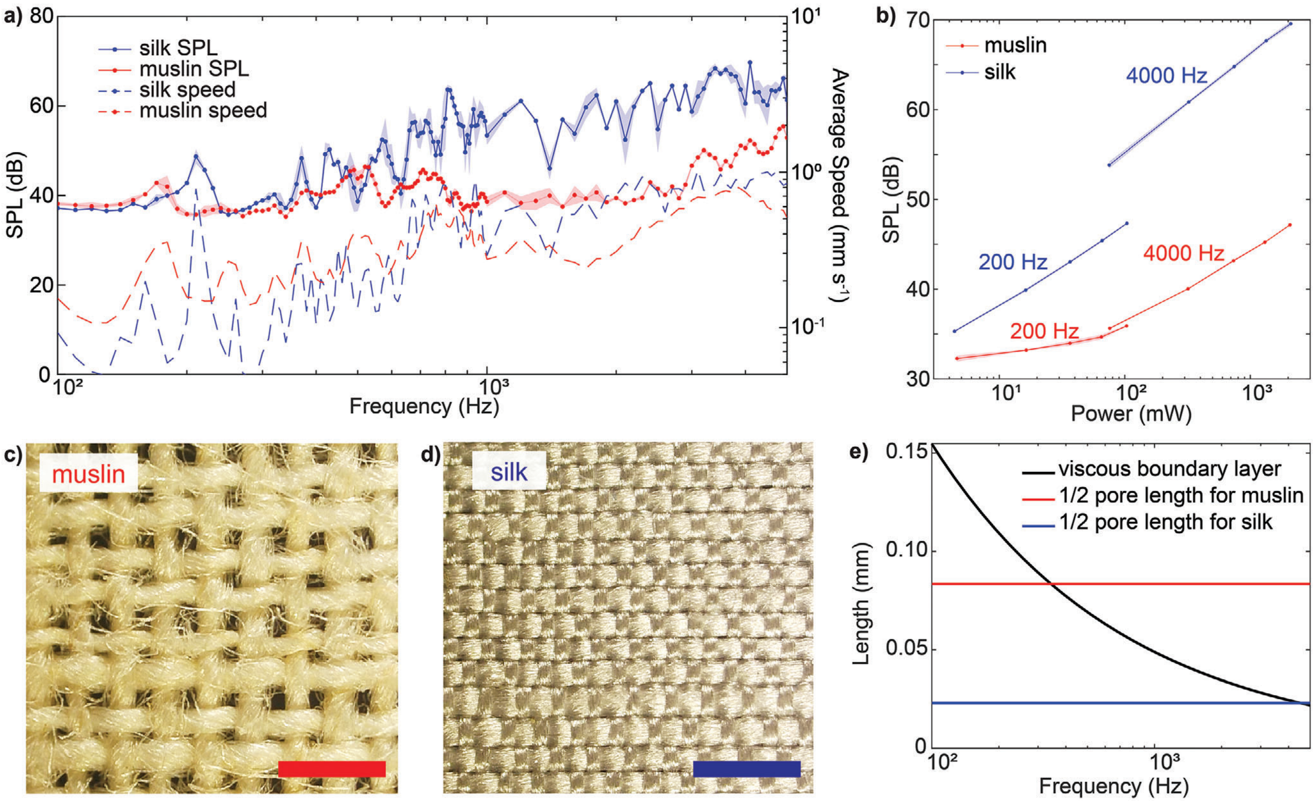

Figure 4. a) SPL and average speed over the surface of the fabrics at frequencies from 100 to 5000 Hz. b) Linear relationship between acoustic pressure and power at different frequencies for both muslin and silk. The noise floor is around 32 dB, so that is the lowest SPL recorded. Optical microscopy images of c) muslin and d) silk. Scale bars are 1 mm. e) Theoretical thickness of the viscous boundary layer compared with the half pore length for muslin and silk.

for direct acoustic suppression, also known traditionally as "active noise cancellation."[34] In many instances, direct acoustic suppression can save material costs and space while providing greater attenuation, particularly at lower frequencies compared to passive noise reduction using sound-absorbing panels.[24,34] The fabric emitter can function as a direct acoustic suppression device by emitting sound waves that destructively interfere with the sound waves of the unwanted noise (Figure 5c).

For the direct acoustic suppression measurement, the reference loudspeaker plays the unwanted noise to be canceled. We will refer to the SPL measured when the sound is only generated by the reference loudspeaker and no voltage is applied to the fiber as "passive SPL." The "active SPL" is when both the reference loudspeaker and the fabric emitter are turned on. The SPL at the point of the reference microphone is minimized when the passive SPL is equal to the generated SPL from the fabric emitter and the sound waves are out of phase. The average sound transmission loss (i.e., the difference between the active and passive SPL) is 19.7 dB (**Figure 6a**). The fabric emitter effectively reduces sound that is as loud as 65 dB all the way to the noise floor, showing promise for reducing noise in larger spaces using distributed panel active noise reduction.

Direct acoustic suppression using just one speaker only achieves sound reduction at particular points in space. While the acoustic pressure can be driven to zero at the point of cancellation, reductions of more than 10 dB are usually only achieved within a distance from the microphone of about one-tenth of a wavelength.[6] To achieve suppression of noise that originates from multiple sources or encounters many points of reflection in a room, complex algorithms and multiple acoustic sources distributed in space must be employed.[10] Because direct acoustic suppression only works locally, limiting the transmission of sound into a volume is a way to reduce the noise in the entire volume.[24,35]

6. Vibration-Mediated Suppression

In order to effectively limit acoustic transmission into a space, the structural vibrations which are transmitting the sound must be controlled. Active structural acoustic control or vibration-mediated suppression involves directly controlling the vibrations of a structure with the objective of reducing overall sound radiation.[10] Just as Figure 5a illustrates sound being transmitted through the motion of the fabric, if the fabric is forced to remain still through some mode of control, the vibrations will be suppressed and the sound will not be transmitted (Figure 5d). By suppressing the vibrations of a fabric, the radiated structure-borne sound will also be suppressed, turning the fabric into an active sound barrier. This control is achieved through the fiber which excites the fabric so that, in isolation, it would generate

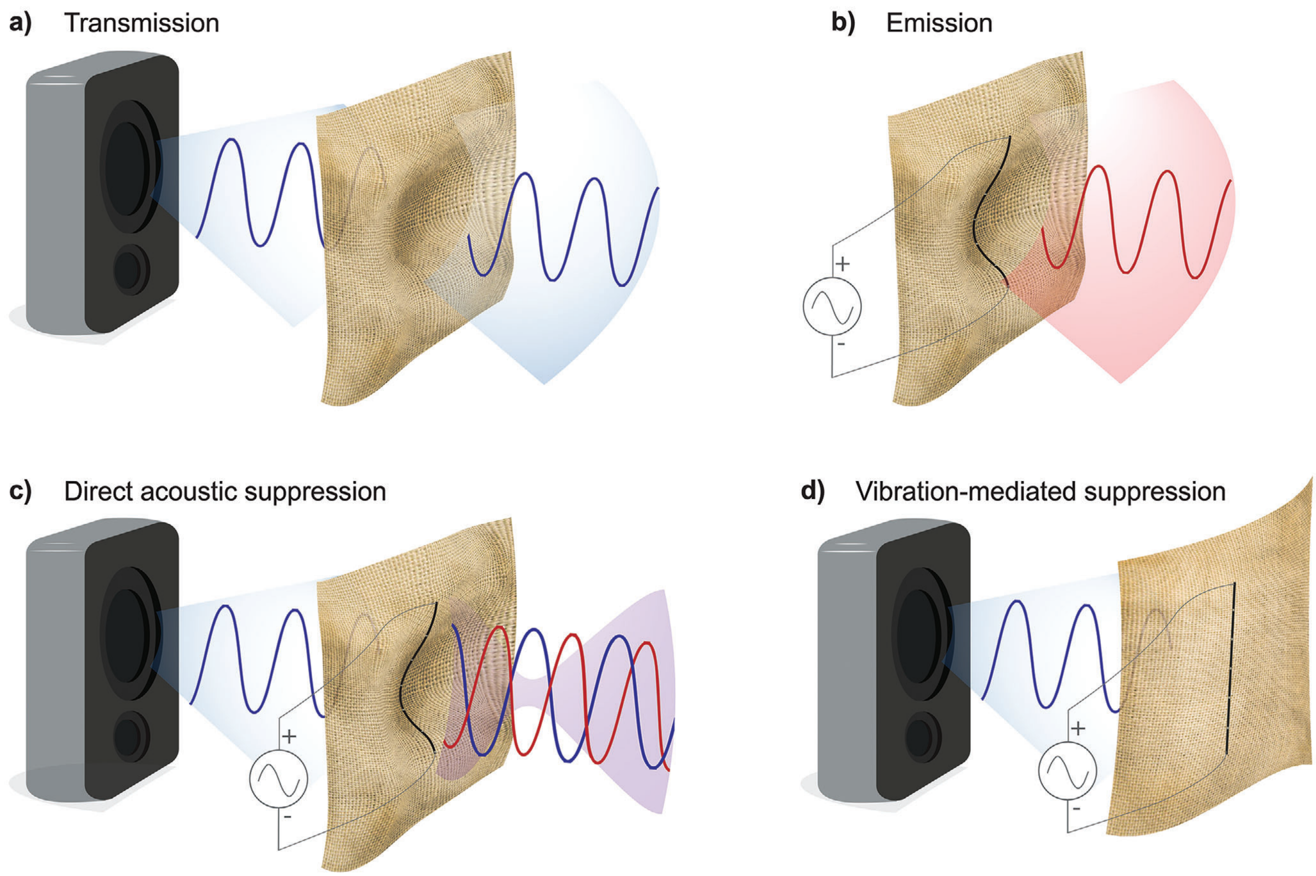

Figure 5. a) In transmission mode, incoming sound waves give rise to vibrations in a passive fabric. These vibrations transfer energy to the air in the form of sound. b) The piezoelectric fiber in the fabric causes the fabric to vibrate, leading to the emission of sound. c) Sound waves resulting from the sound which is transmitted through the fabric interfere with sound waves induced by the piezoelectric fiber vibrating the fabric. This interference can cause the cancellation of the sound at a particular point in space. d) The piezoelectric fiber induces mechanical vibrations that destructively interfere on the surface of the fabric with those induced by the incoming sound waves, subduing the fabric surface and precluding sound transmission through it.

displacement patterns that are equal and opposite to those that would arise from just the incoming pressure wave acting on the fabric. Instead of the fabric being displaced and transmitting the incoming sound, the fabric remains still and becomes an acoustically reflective structure.

There has been research into actively vibrating walls or windows to reduce noise as close as possible to the point at which it enters a room; researchers have explored using larger area acoustic transducers for these applications, such as transparent PVDF polymer membranes[23,36] and elastomeric membranes,[24,37] speakers positioned between double-glazed windows,[38,39] and thin glass panels[40] that can be actively controlled. However, endowing existing structures with active vibration suppression functionality, as in the case of the additional panels or the speaker in between double-glazed windows, is costly and at times infeasible, prompting the need for solutions that treat the problem at the surface. Membrane devices address this challenge but require a large area of active material which can cause challenges in terms of manufacturability and cost-effectiveness. By contrast, the fabric emitter uses traditional fabric materials and a single fiber transducer.

Furthermore, none of these previous studies has shown the suppression of mechanical waves on the surface of the structure of interest.[23,24,36–40] Active vibration suppression on a surface is only effective if the surface itself can excite identical vibrational modes to those excited by the incoming unwanted sound. The vibrational modes excited by a plane pressure wave could differ substantially from the modes excited by the transducer through its specific actuation method. In this study, a single fiber excites complex vibrational modes in the fabric which are identical to those excited by an external pressure wave. To our knowledge, this is the first study to show vibration-mediated suppression substantiated by both SPL and surface vibration measurements. It is also the first study that explores modulating the acoustic reflectivity of fabrics.

To suppress the mechanical vibrations on the surface of the fabric, the fabric should generate vibration patterns that are similar to those generated on the surface of the fabric from an external sound source. The vibration modes are dictated by the geometry, boundary conditions, and mechanical properties of the fabric/fiber assembly. Because the fiber is long enough relative to the diameter of the fabric, it can

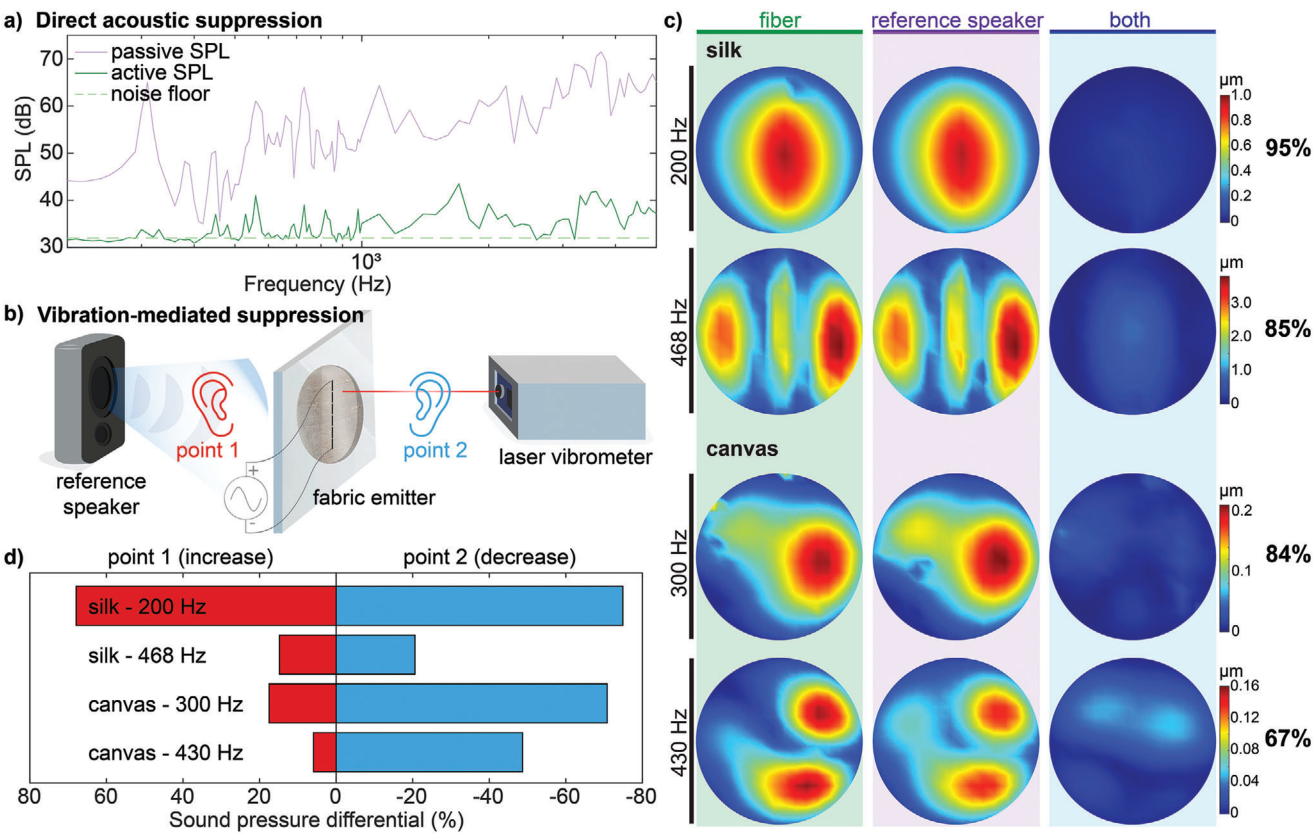

Figure 6. a) Direct acoustic suppression results: passive and active SPL as measured by the reference microphone. The noise floor is 32 dB. b) Vibration-mediated suppression measurement setup. Reference microphones are placed at point 1 and point 2. c) Measured displacement of the fabric surface, showing suppression of the vibrations, with the average displacement reduction percentages listed on the right. d) Percent changes in sound pressure as measured by the microphones at point 1 and point 2 as the fabric switches from passive to active in vibration-mediated suppression mode. The increase at point 1 indicates the increase in reflected sound off the fabric, and the decrease at point 2 indicates the decrease in sound transmitted through the fabric.

induce vibrations over the whole fabric. Thus, the vibration patterns are generally agnostic to the source of excitation, whether it is the fiber or the reference speaker. This consistent matching enables efficient suppression of surface vibrations over the entire surface of the fabric by simply adjusting the phase and relative amplitude of the fiber transducer.

The setup is similar to that used for the direct acoustic suppression demonstration using a reference loudspeaker and the fabric emitter positioned along the wall of acoustic foam. The vibrations of the fabric are measured using the scanning laser vibrometer and two reference microphones are used to measure the SPL at point 1 and point 2 (Figure 6b). The displacement patterns are measured first for the fiber alone exciting the fabric, then for the reference loudspeaker alone exciting the fabric. Finally, the phase and relative volume of the fabric emitter and reference loudspeaker are adjusted so that the amplitude of vibrations is minimized, resulting in up to a 95% reduction in the average surface displacement at the fundamental frequency (Figure 6c) and suppression of at least 67% at other frequencies, using both silk and canvas fabrics. In addition to the results shown here, additional measurements have substantiated pattern matching at other frequencies (Figure S13, Supporting Information). As the sound pressure generated by the fabric is proportional to the average magnitude of displacement of the fabric surface, a 95% reduction in vibration amplitude leads to a 95% reduction in sound pressure in theory.[8] This linear relationship between the amplitude of vibration and the SPL was confirmed through measurements for both silk and canvas, as shown in Figure S14 (Supporting Information). The measured reduction in sound pressure is 75% in this case, as shown by the point 2 sound pressure differential in Figure 6d. The discrepancy between theory and measurement arises from the imperfect isolation of the reference speaker by the acoustic foam, allowing some sound to leak through the foam wall and be picked up by the reference microphone.

With the incident sound unable to impart motion to the fabric, the acoustic reflectivity of the fabric is effectively increased. In contrast with the typical structural acoustic process, when the external sound wave impacts the fabric, the energy is not propagated throughout the fabric. Thus, vibrations do not arise, so the energy is not radiated from the fabric on either side. The external sound is unable to impart motion to the fabric, and so the sound is reflected back. This is substantiated by the SPL measurements that show an increase in sound pressure on the side of the unwanted noise at point 1, while the SPL decreases on the other side

(Figure 6d). The increase in SPL cannot be attributed to emission from the fabric emitter, because its vibration magnitude and thus SPL are substantially decreased. This suggests that the fabric becomes more acoustically reflective when operating in this mode, with measurements indicating that up to 68% of the unwanted sound is reflected back. Previous work in literature describes using a dielectric membrane for active noise control by tuning the tension so that there will be an antiresonant peak at the frequency of the unwanted noise.[41] Thus, the unwanted noise would impact the membrane and, unable to impart any energy to it, be reflected back.[41]

7. Conclusions

Reducing unwanted noise persists as a significant challenge encountered in daily life. Despite its prevalence, current strategies to abate unwanted noise are deficient. This study demonstrates using traditional fabric materials with a piezoelectric fiber device as sound emitters that have applications in sound reduction. Multifrequency sound emission is demonstrated from a woven fabric with fixed and free boundary conditions. The mechanical properties that govern the vibration of thin plates similarly affect the vibration patterns in the fabric emitters generated by the fiber. Additionally, the pore size influences the fabric's sound emission efficiency as fabric emitters can undergo losses through pores that are relatively large compared to the viscous boundary layer, as illustrated by the responses of muslin and silk. Two strategies are employed to demonstrate using fabrics for active sound control. First, direct acoustic suppression is demonstrated through the destructive interference of sound waves in air, and the 0.13 mm thick silk fabric effectively cancels sound up to 65 dB. To reduce sound not just at a particular point but to prevent it from entering a space, vibration-mediated suppression can be used. This study demonstrates reducing the vibrations on the surface of a fabric up to 95%, leading to a 75% reduction in the transmitted sound. The vibration-mediated suppression is enabled by the vibrational modes on the fabric excited by the fiber matching with those excited by the external sound source. At the right relative phase, when the external sound wave impacts the fabric, the energy is not imparted to it, and the sound wave is reflected back. In order to suppress multifrequency sound waves originating from multiple sources, advanced signal processing and the development of complex control algorithms will be needed for the applications of both direct acoustic suppression and vibration-mediated suppression to be feasible in real-world scenarios. There is opportunity to face this challenge by using the additional degrees of freedom that the fabric emitter system offers, as multiple fibers and fabrics of various sizes and orientations could be used in a single system to suppress more complex sound. Despite being thin, lightweight, and porous materials, fabrics can be transformed into effective sound emitters for a variety of acoustic applications, including active barriers that prevent sound from entering a space.

8. Experimental Section

Poling: The fibers were immersed in castor oil heated to 65–70 °C and undirectionally poled using a step-wise poling method, similar to that described previously.[17] The voltage was increased in increments of 100 V, following the pattern of voltage on for 4 min and voltage off for 3 min, until the voltage that gave a field strength of ≈133 MV m^{-1} was reached. The poling process lasted 6.5 h before removing the voltage and returning the fibers to room temperature.

Electric Displacement–Electric Field Hysteresis (D–E) Loop Measurements: *D–E* loop measurements were conducted at room temperature for the samples poled at different fields. A Premiere II ferroelectric tester (Radiant Technologies, Inc., Albuquerque, NM) and a Trek 10/10B-HS high-voltage amplifier (0–10 kV AC, Lockport, NY) were used. The output voltage had a bipolar sinusoidal waveform of ±100 MV m^{-1} at 1 Hz. Both the first and second loops were recorded after poling. The samples were immersed in silicone oil to avoid possible corona discharge in air.

Emitter Sample Preparation: Three different fabrics were used: muslin (OnlineFabricStore, Unbleached Muslin Fabric, 1814), canvas (OnlineFabricStore, #4 Natural Cotton Duck Fabric, DUCK460), and silk (OnlineFabricStore, Silk Shantung Fabric SH-1577). Each fabric was ironed and then lightly tensioned in an embroidery hoop. A 6.7 cm acoustic fiber was then stitched onto the center of the fabric. An acrylic ring was epoxied to the face of the fabric and then it was set upside down for 24 h. Then, a 11 cm outer diameter, 8 cm inner diameter, 1.5 mm thick acrylic ring was epoxied on the back. An 11 cm diameter acrylic plate and a 200 g weight placed on top provided the force of tension while the epoxy cured for 24 h. The ring was then cut out of the excess fabric and placed in a metal frame. The Mylar (Goodfellow, polyethylene terephthalate–metallized film, ES30-MZ-000255) membrane loudspeaker was made in the same process without the ironing and embroidery hoop, and the acoustic fiber was fastened to the surface with a thin layer of glue.

Sound Pressure Level Measurements: A function generator (Rigol, DG1022), which generated the signal that the fabric speaker would output, was connected to an amplifier (Crown, DC-300A Series II) and then an audio transformer (Hammond Mfg., 1650R), which passed the signal to the fiber. A multimeter (Fluke, 189) was connected in series with the fiber to measure current. A reference microphone (MiniDSP, UMIK-2) was positioned at the center of the sample either 2.5 or 30 cm away from the fiber, for near-field and far-field measurements, respectively. The SPL was recorded from the reference microphone using Room EQ Wizard Room Acoustics Software (REW). SPL was measured in A-weighted decibels. A schematic of the electronics setup is shown in Figure S15 (Supporting Information).

Vibrometer Measurements: A scanning laser vibrometer (Polytec PSV-500 Scanning Vibrometer) was used in Fast Fourier Transform (FFT) or FastScan mode to measure the velocity over the surface of the fabric at specific frequencies.

Direct Acoustic Suppression Measurements: A commercial reference loudspeaker (PreSonus, ERIS E3.5) was positioned 30 cm away from the silk fabric on the other side of an acoustic foam partition with an opening in it at the site of the fabric. The reference microphone (MiniDSP, UMIK-2) was positioned 2.5 cm away on the opposite side. The phase and relative volume of the fiber was tuned such that the SPL measured by the reference microphone was minimized.

Vibration-Mediated Suppression Measurements: A commercial reference loudspeaker (PreSonus, ERIS E3.5) was positioned 30 cm away from the silk fabric on the other side of an acoustic foam partition with an opening in it at the site of the fabric. Two reference microphones (MiniDSP, UMIK-2) were placed 3 cm away from the fabric on either side. The displacement of the fabric that arose from the sound of the reference loudspeaker was measured using the laser vibrometer. Next, the displacement of the fabric that arose from applying a voltage to the fiber was also measured using the laser vibrometer. The voltage applied to the fiber was then adjusted to achieve the same average magnitude of displacement in each case, following the linear relationship between voltage and displacement at each frequency (Figure S14, Supporting Information). Then, a point of maximum displacement was chosen and the phase of the reference loudspeaker was tuned such that the displacement measured by the laser vibrometer (Polytec PSV-500 Scanning Vibrometer) was minimized.

Specific Flow Resistance Measurements: The specific flow resistance was measured for all of the fabrics using a constant pressure–variable volume permeation apparatus. To prevent leakage from the upstream to downstream within the permeation cell, all samples were secured onto brass supports using epoxy adhesive. A constant pressure of N_2 gas was supplied at room temperature in the upstream, and the downstream flow rates were measured using a digital mass flow meter (Aalborg Instruments, XFMS-010652).

Fabric Modulus Measurements: Rectangular samples of fabric were cut along the warp and weft directions. The yarns in the long direction were unraveled for 0.5 cm on each side, leaving the center 1 cm of fabric intact. This was done to mitigate edge effects during the measurement (Figure S16a, Supporting Information). Tensile testing of the fabric pieces was performed at a rate of 1.2 mm min^{-1} using an Instron Corporation 8848 MicroTester. The modulus was calculated by taking the average slope of multiple tests (Figure S16b–d, Supporting Information).

COMSOL Simulation: The COMSOL simulation consisted of two studies, both in the frequency domain. The geometry was simplified so that the fiber was modeled as a block (67 × 1.25 × 0.691 mm) and the fabric was modeled as an 8 cm thin cylinder or plate. The fabric was surrounded by air that was bordered by a perfectly matched layer (PML). Pressure Acoustics physics was applied to the air and PML domains. Structural Mechanics physics was applied to the fiber. Poroelastic Waves physics was applied to the fabric. The first, a background pressure field of 30 Pa was used to generate the motion in the fabric. In the second study, the background pressure field was disabled and the prescribed displacement of the fabric was set to be the resultant displacement from the first study. The acoustic pressure field was generated from this displacement and the SPL was taken at a point 2.5 cm away axial from the center of the fabric. The model inputs were the thickness, Young's modulus, density, Poisson's ratio, porosity, specific flow resistance, and isotropic loss factor. The isotropic loss factor and Poisson's ratio were assumed to be 0.001 and 0.49, respectively.[42] The porosity and specific flow resistance were measured to be 0.56 and 0.462 bar s m^{-1}, respectively, and those values were used in the simulation. The thickness and density were set to 1.1 mm and 620 kg m^{-3}, which were 4% and 9%, respectively, less than the measured values. The Young's modulus was chosen to be 210 MPa, which was higher than the measured modulus of 140 MPa. This increase was justified as there was some tension applied to the fabric in the frame, which was unaccounted for in the model, and would provide another restoring force to the vibrating fabric, in addition to the fabric's stiffness.

Supporting Information

Supporting Information is available from the Wiley Online Library or from the author.

Acknowledgements

The authors would like to thank David Bono from the MIT for his contributions to the electronics setup; Dr. Mark Cops from the COMSOL for his support of the simulations; David Damiani, Ryan Graham, and Jack Danieli from the Polytec for assistance in setting up and processing the vibrometer measurements; Shane Campbell for carrying out the stress–strain measurements.Research was sponsored by the Army Research Office and was accomplished under Cooperative Agreement Number W911NF-18-2-0048 and Cooperative Agreement Number W911NF-23-2-0121. The views and conclusions contained in this document are those of the authors and should not be interpreted as representing the official policies, either expressed or implied, of the Army Research Office of the U.S. Government. The U.S. Government is authorized to reproduce and distribute reprints for Government purposes notwithstanding any copyright notation herein. G.H.Y., H.C., Y.Z., and Y.F. acknowledge support by DTRA (Award No. HDTRA1-20-2-0002) Interaction of Ionizing Radiation with Matter (IIRM) University Research Alliance (URA); G.H.Y. acknowledges the funding support from the National Science Foundation Graduate Research Fellowship under Grant No. 2141064; J.L. and C.M. acknowledge the funding support from the National Science Foundation Grant No. CCSS-2237619 and the Wisconsin Alumni Research Foundation; L.Z. acknowledges the funding support from Grant No. NSF/DMR-2103196.

Conflict of Interest

The authors declare no conflict of interest.

Data Availability Statement

The data that support the findings of this study are available in the supplementary material of this article.

Keywords

active noise canceling, fabric, fiber, flexible loudspeaker, piezoelectric

Received: December 7, 2023
Revised: March 28, 2024
Published online:

[1] *Environmental Noise Guidelines for the European Region*, WHO Regional Office For Europe, Copenhagen, Denmark **2018**.
[2] E. Baumgaertner, J. Kao, E. Lutz, J. Sedgwick, R. Taylor, N. Throop, J. Williams, *N. Y. Times* **2023**.
[3] M. T. Osborne, A. Radfar, M. Z. O. Hassan, S. Abohashem, B. Oberfeld, T. Patrich, B. Tung, Y. Wang, A. Ishai, J. A. Scott, L. M. Shin, Z. A. Fayad, K. C. Koenen, S. Rajagopalan, R. K. Pitman, A. Tawakol, *Eur. Heart J.* **2020**, *41*, 772.
[4] S. A. Stansfeld, M. P. Matheson, *Br. Med. Bull.* **2003**, *68*, 243.
[5] M. S. Hammer, T. K. Swinburn, R. L. Neitzel, *Environ. Health Perspect.* **2014**, *122*, 115.
[6] S. J. Elliot, P. A. Nelson, *IEEE Signal Process. Mag.* **1993**, *10*, 12.
[7] M. A. Kuczmarski, J. C. Johnston, *Acoustic Absorption in Porous Materials*, NASA Glenn Research Center, Cleveland, OH **2011**.
[8] L. Kinsler, A. Frey, A. Coppens, J. Sanders, *Fundamentals of Acoustics*, John Wiley & Sons, Inc., New York, NY **2000**.
[9] Acoustic Insulation Market by Material Type, **2022**.
[10] C. C. Fuller, S. Elliott, P. A. Nelson, *Active Control of Vibration*, Academic Press, San Diego **1996**.
[11] J. H. Lee, K. H. Cho, K. Cho, *Adv. Mater.* **2023**, *35*, 2209673.
[12] C. Zhi, S. Shi, Y. Si, B. Fei, H. Huang, J. Hu, *Adv. Mater. Technol.* **2023**, *8*, 2201161.
[13] N. Gao, Z. Zhang, J. Deng, X. Guo, B. Cheng, H. Hou, *Adv. Mater. Technol.* **2022**, *7*, 2100698.
[14] Z. Lin, S. Duan, M. Liu, C. Dang, S. Qian, L. Zhang, H. Wang, W. Yan, M. Zhu, *Adv. Mater.* **2023**, *36*, 2306880.
[15] S. Egusa, Z. Wang, N. Chocat, Z. M. Ruff, A. M. Stolyarov, D. Shemuly, F. Sorin, P. T. Rakich, J. D. Joannopoulos, Y. Fink, *Nat. Mater.* **2010**, *9*, 643.
[16] N. Chocat, G. Lestoquoy, Z. Wang, D. M. Rodgers, J. D. Joannopoulos, Y. Fink, *Adv. Mater.* **2012**, *24*, 5327.
[17] W. Yan, G. Noel, G. Loke, E. Meiklejohn, T. Khudiyev, J. Marion, G. Rui, J. Lin, J. Cherston, A. Sahasrabudhe, J. Wilbert, I. Wicaksono, R. W. Hoyt, A. Missakian, L. Zhu, C. Ma, J. Joannopoulos, Y. Fink, *Nature* **2022**, *603*, 616.
[18] W. Li, D. Torres, R. Díaz, Z. Wang, C. Wu, C. Wang, Z. L Wang, N. Sepúlveda, *Nat. Commun.* **2017**, *8*, 15310.

[19] J. Han, J. Lang, V. Bulovic, *IEEE Trans. Ind. Electron.* **2022**, *70*, 985.
[20] T. Sugimoto, K. Ono, A. Ando, K. Kurozumi, A. Hara, Y. Morita, A. Miura, *Appl. Acoust.* **2009**, *70*, 1021.
[21] X. Qiu, G. C. Schmidt, P. M. Panicker, R. A. Quintana Soler, A. J. Benjamin, A. C. Hübler, *Adv. Eng. Mater.* **2019**, *21*, 1900537.
[22] K. R. Lee, S. H. Jang, I. Jung, *Nanotechnology* **2018**, *29*, 325502.
[23] X. Yu, R. Rajamani, K. A. Stelson, T. Cui, *Sens. Actuators, A* **2006**, *132*, 626.
[24] P. Rothemund, X. P. Morelle, K. Jia, G. M. Whitesides, Z. Suo, *Adv. Funct. Mater.* **2018**, *28*, 1800653.
[25] H. Dsouza, A. Van Schyndel, J. Pastrana, Y. Cao, E. Hunter, B. Rakerd, N. Sepúlveda, *J. Sound Vib.* **2020**, *468*, 115091.
[26] H. Y. Chiang, Y. H. Huang, *Appl. Acoust.* **2018**, *129*, 365.
[27] A. Yildirim, J. C. Grant, G. Song, S. H. Yook, Z. Mutlu, S. Peana, A. Dhanabal, S. K. Sinha, R. Daniels, K. M. Bellisario, G. A. Sotzing, D. H. Huston, B. C. Pijanowksi, R. Rahimi, Y. Liu, M. Cakmak, *Adv. Mater. Technol.* **2020**, *5*, 2000296.
[28] H. Wang, Y. Ma, Q. Zheng, K. Cao, Y. Lu, H. Xie, *Micromachines* **2021**, *12*, 1257.
[29] M. Shehzad, S. Wang, Y. Wang, *npj Flexible Electron* **2021**, *5*, 21.
[30] J. P. Fay, S. Puria, C. R. Steele, *Proc. Natl. Acad. Sci. USA* **2006**, *103*, 19743.
[31] C. Rawlins, *Basic AC Circuits*, Newnes, Boston **2000**.
[32] J. W. S. Hearle, P. Grosberg, S. Backer, *Structural Mechanics of Fibers, Yarns, and Fabrics*, Wiley-Interscience, NY, USA **1969**.
[33] M. Yang, P. Sheng, *Annu. Rev. Mater. Res.* **2017**, *47*, 83.
[34] J. E. F. Williams, *Proc. R. Soc. London, Ser. A* **1984**, *395*, 63.
[35] F. J. Fahy, P. Gardonio, *Sound and Structural VIbration: radiation, transmission, and response*, Academic Press, Boston **2007**.
[36] J. Lane, *Active Control of Noise through Windows*, University of Canterbury, New Zealand **2013**.
[37] Z. Lu, Y. Cui, M. Debiasi, *Appl. Acoust.* **2016**, *111*, 39.
[38] O. E. Kaiser, S. J. Pietrzko, M. Morari, *J. Sound Vib.* **2003**, *263*, 775.
[39] A. Jakob, M. Möser, *Appl. Acoust.* **2003**, *64*, 163.
[40] H. Zhu, X. Yu, R. Rajamani, K. A. Stelson, *Mechatronics* **2004**, *14*, 805.
[41] K. Jia, M. Wang, T. Lu, J. Zhang, T. Wang, *Smart Mater. Struct.* **2016**, *25*, 055047.
[42] H. Sun, N. Pan, R. Postle, *Compos. Struct.* **2005**, *68*, 505.